Volume 1 | Number 1 | Jan 2013 | Pages 1–100

Dalton Transactions

An international journal of inorganic chemistry
www.rsc.org/dalton

ROYAL SOCIETY OF CHEMISTRY

ROYAL SOCIETY OF CHEMISTRY

www.rsc.org/dalton

Journal Name

ARTICLE TYPE

Novel Ce³⁺ activated Lu₃MgAl₃SiO₁₂ garnet phosphor for blue chip light-emitting diodes with excellent performance

Yurong Shi, [a,b] **Ge Zhu,** [a] **Masayoshi Mikami,** [c] **Yasuo Shimomura** [c] **and Yuhua Wang*** [a]

A novel Ce³⁺ activated Lu₃MgAl₃SiO₁₂:Ce phosphor was synthesized and found to crystallize in the garnet structure. The crystal structure of synthesized phosphors has been characterised by X-ray diffraction and refined with Rietveld refinements. Both room and high temperature photoluminescence spectra are utilized to investigate the luminescence properties and crystal field splitting. The high

10 temperature quenching of these phosphors and quantum efficiency (QE) are also studied using both the prepared YAG:Ce and commercial YAG:Ce phosphor named P46-y3 as reference. Upon excitation by blue light, the composition-optimized Lu₃MgAl₃SiO₁₂:Ce phosphor exhibited strong yellow light with a high QE of 81.2% and better thermal stability than that of commercial phosphor. The results indicate that Lu₃MgAl₃SiO₁₂:Ce phosphor can serve as a candidate phosphor for blue chip LEDs.

15 1.   Introduction

The development of efficient white light-emitting diodes (*w*-LEDs) has provided tremendous potential in reducing energy use by replacing conventional lighting source, such as fluorescent or incandescent lamps.[1-4] The most common method to create white

20 light is partially converting the blue light from InGaN chip in Y₃Al₅O₁₂:Ce³⁺ (YAG:Ce) phosphor to yellow. Although the path of white light realization is inexpensive and efficient, it has poor color rendering properties due to the deficiency of the red component limiting its application in some field,[5-7] like in-home

25 lighting which takes up the majority of the lighting market. To meet the requirements for general illumination lighting, two major modifications have been developed. One is the modification of the YAG:Ce system, including co-doping rare earth ions (Pr³⁺, Sm³⁺, Eu³⁺, etc.) [8-10] or transition metal ions

30 (Mn²⁺),[11] which could increase red component, as well as substituting host components by other ions (Y³⁺ substituting by Tb³⁺, Gd³⁺, [9,10,12,13] Al³⁺ substituting by Mg²⁺-Si⁴⁺ or Mg²⁺-Ge⁴⁺,[14] and O²⁻ substituting by N³⁻,[6] etc.) to change the crystal field strength or covalence. The problem is the enhancement of

35 the red component efficiency is not obvious, and almost all bright and thermal stability of modification YAG:Ce is obviously declined. The other is exploring novel red phosphors which are usually based on Eu²⁺ doped nitride [15,16] phosphors. However, these phosphors require critical preparation conditions like high

40 temperature, high pressure and expensive raw materials, etc. Besides, they have to be blended with YAG:Ce phosphor to make white lamps, possibly leading to variations during lamp manufacturing. In principle, using a single phosphor rather than two or three could help to reduce sort of this variability.

45 The host of commercial YAG:Ce phosphor belongs to garnet structure, and currently, garnet structure is almost the only oxide host for Ce³⁺ doped that could absorb blue light and emit from green-yellow to orange-red light. [5,17-23] The general stoichiometric formula of the garnet structure is {A}₃[B]₂(C)₃O₁₂, where A, B

50 and C are dodecahedral, octahedral and tetrahedral coordination, respectively. In this structure, Ce³⁺ occupies A site and emits from green to orange light through varying crystal field strength and covalent characteristic, because the energy position of the lowest Ce³⁺ 5d level could be justified by changing the crystal

55 field strength around Ce³⁺ and the covalency of Ce³⁺-O²⁻. Thus, it is possible and valid to modify the typical garnet composition to obtain a significant red-shift emission spectrum by enhancing the crystal field strength surrounding of Ce³⁺ or decreasing covalent interaction between the oxygen anions and A ions (A³⁺-O²⁻). In

60 principle, an increased diameter of the A site results in an increased crystal field strength of Ce³⁺. In contrast, an increase in the average diameter of B or C sites results in a decrease covalent interaction between A³⁺-O²⁻.[5] These provide a simple design rules for Ce³⁺ luminescence in garnet hosts. For example, Mg²⁺-Si⁴⁺

65 substitution on the B and C sites, respectively, leads to Ce³⁺ emission band shift to the longer wavelength. However, further red shift of the emission is limited by garnet phase instability due to the competition of apatite structure forming, and leads to lower efficiencies at room temperatures.[5] As a consequence, there are

70 rare reports on larger amount substitution of Mg²⁺-Si⁴⁺ pairs in YAG:Ce. However, smaller dodecahedral A cations substitution can strengthen the garnet phase stability.[24] Under the guidance of above principles, if we induce larger amount Mg²⁺-Si⁴⁺ pairs into YAG host, smaller Lu³⁺ should be put in place to substitute Y³⁺ to

75 keep stability. In other words, Lu³⁺ based garnet host Lu₃MgAl₃SiO₁₂ should be more stable than Y³⁺ based Y₃MgAl₃SiO₁₂,[24] and Ce³⁺ activated Lu₃MgAl₃SiO₁₂ could be expected with better luminescence properties (Shown in Figure S1-S3).

In a practical sense, phosphors should not only have redder spectra for lower correlated color temperature (CCT) and high color rendering index (CRI) but also have high QE and thermal stability for warm white LED phosphors. The aim of this work is to investigate Ce^{3+} activated $Lu_3MgAl_3SiO_{12}$ garnet phosphor, and discuss its synthesis, crystal structure and luminescence properties in w-LEDs use.

2. Experimental methods

Using the conventional high temperature solid-state reaction method $Lu_3MgAl_3SiO_{12}$:xCe ($Lu_{3-x}Ce_xMgAl_3SiO_{12}$, x=0.04, 0.06, 0.07, 0.08, 0.09, 0.10) phosphors were prepared. The starting materials (Lu_2O_3, 99.99%, CeO_2, 99.99%, $4MgCO_3\cdot Mg(OH)_2 \cdot 5H_2O$, A.R., Al_2O_3, A.R. and H_3SiO_4, A.R.) were all weighed out as the desired stoichiometry and thoroughly mixed using an agate mortar with small amount of ethanol. The mixtures were first fired using BN crucibles at 800℃ for 2h then at 1500℃ for 6h in 5% H_2 + 95% N_2 atmosphere. Finally, the samples were cooled to room temperature in the furnace, and then ground in an agate mortar. All samples are yellow body color. YAG:Ce was also synthesized as a reference by solid-state reaction with 1 wt% BaF_2 as flux at 1500℃ for 6h in 5% H_2 + 95% N_2 atmosphere.

Powder X-ray diffraction (XRD) data were collected on a Rigaku D/MAX-2400 powder X-ray diffractometer with Cu Kα radiation ($\lambda = 1.54178$ Å) operating at 40 kV and 60 mA. Step scans were performed from 5 to 110° 2θ and a step size of 0.02. Generally, refined lattice parameters of XRD patterns were fitted by Rietveld refinements using Maud software. Excitation (PLE) and emission (PL) spectra were measured by HORIBA JOBIN YVON Fluorlog-3 spectrafluorometer system. The QE was measured by a FLS-920T fluorescence spectrophotometer. High temperature luminescence intensity measurements were carried out by using an aluminum plaque with cartridge heaters; the temperature was measured by thermocouples inside the plaque and controlled by a standard TAP-02 high temperature fluorescence controller. All measurements are taken at room temperature unless otherwise mentioned.

3. Results and Discussion

3.1 Crystal structure analysis of garnet phase

Fig. 1 shows a Rietveld refinement of XRD patterns of $Lu_3MgAl_3SiO_{12}$:0.06Ce phosphor. The initial structural model of the actual structure of $Lu_3MgAl_3SiO_{12}$:0.06Ce phosphor was constructed with crystallographic data previously reported for $Y_3Al_5O_{12}$ (JCPDS Card No. 33-0040). The refinement result shows the pattern matched well with the model regardless of the minor apatite impurity peaks, corresponding to $Ia\bar{3}d$ (No.230) space group, and lattice constants were refined as a = 11.9421 Å. The lattice parameter of $Lu_3MgAl_3SiO_{12}$:Ce phosphor is smaller than YAG (12.066 Å),[6] which is likely due to the smaller size of Lu^{3+} vs Y^{3+}. Nevertheless, it's larger than $Lu_3Al_5O_{12}$ (LuAG, 11.912 Å), due to lager size of Mg^{2+} vs Al^{3+}. The Rietveld refinement of $Lu_3MgAl_3SiO_{12}$:Ce phosphor (Table 1) shows that the 24c, 16a, 24d and 96h Wyckoff sites are occupied by Ce/Lu, Mg/Al1, Si/Al2 and O, respectively. However, occupancies of all ions are slightly less than expected from the nominal composition

of $Lu_3MgAl_3SiO_{12}$:Ce. This is considered due to existing small amount apatite compounds.
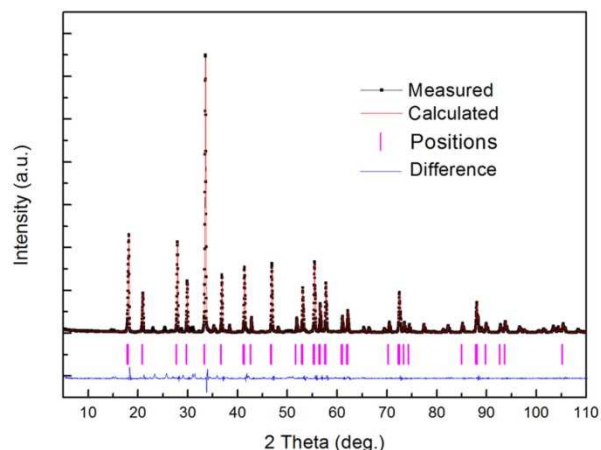

Fig. 1 Measured (black solid line) and calculated (red line) XRD pattern of $Lu_3MgAl_3SiO_{12}$:0.06Ce phosphor with positions of all the reflections (vertical line) and a difference profile (blue line).

Table 1 Refined Structural Parameters for $Lu_3MgAl_3SiO_{12}$:0.06Ce sample.

atom	Wyckoff	x	y	z	occupancy
Lu	24c	0.125	0	0.249	0.874
Ce	24c	0.125	0	0.249	0.0095
Mg	16a	0	0	0	0.652
Al1	16a	0	0	0	0.4538
Si	24d	0.375	0	0.250	0.359
Al2	24d	0.375	0	0.250	0.7047
O	96h	-0.301	0.217	-0.095	1.008

Space group: $Ia\bar{3}d$ (No.230); a = 11.9421 Å; Sig = 2.110, Rw% = 14.90, Rwnb = 11.25, Rb = 8.812, Rexp = 7.065
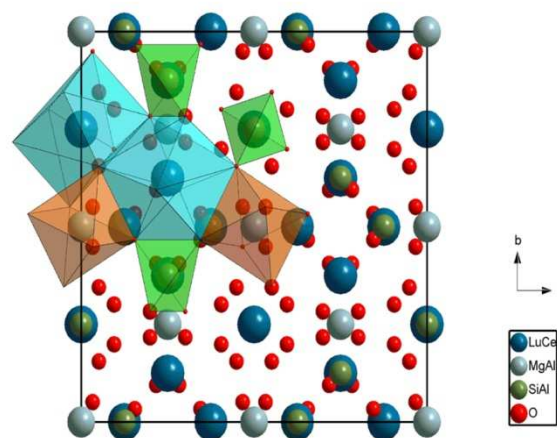

Fig. 2 Crystal structure of $Lu_3MgAl_3SiO_{12}$:0.06Ce phosphor.

A schematic diagram of the $Lu_3MgAl_3SiO_{12}$:0.06Ce garnet structure according to the Rietveld refinement is displayed in Fig. 2. Ce/Lu are randomly distributed on the dodecahedral sites, shown in blue color; Mg/Al1 are randomly distributed on the octahedral sites, shown in orange color, and Si/Al2 are randomly

distributed on the tetrahedral sites, shown in green color. The $(Ce/Lu)O_8$ dodecahedrons are connected with $(Mg/Al1)O_6$ octahedrons by their shared edges, while are connected with part of $(Si/Al2)O_4$ tetrahedrons by one O atom, and the other

5 tetrahedrons by edges. In fact, every $(Ce/Lu)O_8$ dodecahedron is surrounded by four $(Ce/Lu)O_8$ dodecahedron, four $(Mg/Al1)O_6$ octahedrons and six $(Si/Al2)O_4$ tetrahedrons, which means that every coordination O^{2-} of Ce^{3+} is shared by four cations, two Lu^{3+}, one Mg/Al1 and one Si/Al2. Thus, the photoluminescence of Ce^{3+}

10 is not only affected by $(Ce/Lu)O_8$, but also by $(Mg/Al1)O_6$ and $(Si/Al2)O_4$.

To make sure all obtained samples are garnet structure, a quicker scan XRD is used. Fig. 3 shows the XRD patterns of the obtained $Lu_3MgAl_3SiO_{12}:xCe$ phosphors. All samples are in agreement

15 with the garnet structure, and it is hard to find impurity phases under the condition of quicker scan. Combined with Rietveld refinement, we believe that there is bare amount of impurity phases in obtained $Lu_3MgAl_3SiO:xCe$ phosphors. The influence on photoluminescent properties of bare amount of impurity

20 phases will be discussed later. In addition, the activator up to 0.10 does not cause any significant change in the structure.
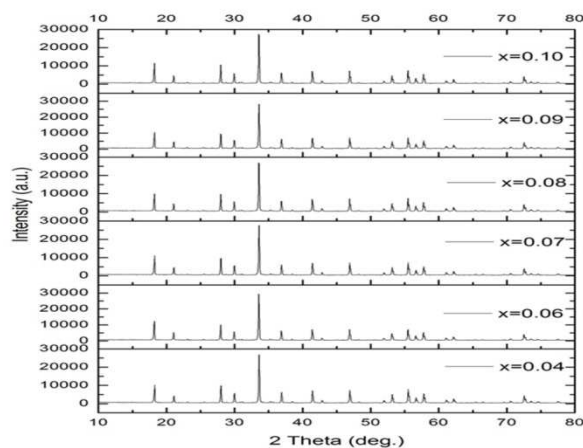

Fig. 3 XRD patterns of $Lu_3MgAl_3SiO_{12}:xCe$ phosphor.

3.2 Luminescence properties of $Lu_3MgAl_3SiO_{12}$:Ce phosphor

25 As expected for a garnet host, the lowest Ce^{3+} $4f^1$-$5d^1$ absorption transition is in the blue spectral region, leading to a green-yellow to orange color. The excitation spectra of $Lu_3MgAl_3SiO_{12}:0.06Ce$ phosphor and com-YAG:Ce (P46-y3) are shown in Fig. 4a. For both phosphors, the spectral was measured for the Ce^{3+} emission

30 band maximum. Both excitation spectral exhibit two excitation bands of Ce^{3+}, one 5d band between 370 nm to 500 nm, and the other 5d band level between 300 nm to 360 nm, which corresponds to the two lowest 5d levels of Ce^{3+} ($5d^1$ and $5d^2$ bands, respectively). The intensity of $5d^2$ band is less than two

35 times as much than that of $5d^1$ band due to symmetry selection rules. [25,26] And the ratio of $5d^1$ band intensity divided $5d^2$ band is 2.80 and 2.73 for $Lu_3MgAl_3SiO_{12}:0.06Ce$ phosphor and P46-y3, respectively. The similar ratio of these two phosphors indicates the same symmetry between $Lu_3MgAl_3SiO_{12}:0.06Ce$ and

40 YAG:Ce phosphors.

It is difficult to analysis of the Ce^{3+} 5d crystal field splitting of $Lu_3MgAl_3SiO_{12}:0.06Ce$ phosphor at room temperature due to the secondary phase excitation bands obscure the higher energy Ce^{3+}

5d levels of garnet, seen the wide band range from 250 nm to 380

45 nm in Fig. 4a. But it is known, Ce^{3+} doped garnet phosphors have much better thermal stability than Ce^{3+} doped silicate apatite or oxysilicate. [27-29] Thus it is possible to obtain pure garnet excitation spectra at higher temperature like 250 °C. According to above, a perfect excitation spectrum was obtained at 250 °C,

50 shown in Fig. 4b. From high temperature excitation spectrum, the splitting between the lowest two Ce^{3+} 5d levels in $Lu_3MgAl_3SiO_{12}:0.06Ce$ phosphor is ~ 7468 cm^{-1}, smaller than that of ~ 7600 cm^{-1} in YAG:Ce, [5] expecting better thermal stability than that of YAG:Ce. However, this is larger than that of

55 LuAG:Ce for ~ 6430 cm^{-1}. [30,31] In Ce^{3+} activated garnet structure, the splitting of the 5d state can be related to a $^2T_{2g}$-^2E_g cubic crystal field splitting with the additional splitting due to the distortion of the cubic coordination into a dodecahedron with D_2 symmetry. [32,33] $Lu_3MgAl_3SiO_{12}:0.06Ce$ phosphor compared with

60 YAG:Ce phosphor, smaller size of dodecahedral Lu^{3+} gives a more cubic environment of Ce^{3+}, resulting in a reduction crystal field strength around Ce^{3+} than Y-based garnet, revealing smaller crystal fields splitting. While compared with LuAG:Ce, Mg^{2+}-Si^{4+} substitution Al^{3+} results in inherent disorder in the host

65 lattice and obtaining stronger crystal fields splitting. [17] Besides, the position of the lowest Ce^{3+} $4f^1$-$5d^1$ absorption transition is at higher energy in $Lu_3MgAl_3SiO_{12}:0.06Ce$ phosphor than YAG:Ce (460 nm), while its very close to that of $Lu_3Al_5O_{12}:Ce^{3+}$ (LuAG:Ce) (~450 nm) phosphor, [30,31] which may be due to the

70 same electronegativity because of the same Lu^{3+} ions in dodecahedral sites.

Excitation into the absorption band at 450 nm gives a typical asymmetric garnet luminescence band with maxima of ~560 nm, although not so red as that for P46-y3, but redder than that for

75 prepared YAG:Ce. The emission is red shifted of ~835 nm compared to non-doped YAG:Ce, shown in Fig. 4c. However, UV excitations lead to the blue emission band. Among the phases present in these samples, Ce^{3+} doped silicate apatite or oxysilicate [27-29] should correspond to the blue region. The deep blue emission

80 from the impurity phases can be absorbed by the garnet in these samples, leading to garnet luminescence and spurious UV peaks in the garnet excitation spectra. In addition, the relative intensity of the blue band compared to garnet yellow band also indicates that Ce^{3+} has reduced solubility in the garnet under these

85 synthesis conditions, supporting the above Rietveld refinement results. Fortunately, Ce^{3+} doped silicate apatite or oxysilicate can barely absorb blue light. Thus the effect of bare amount of impurity phases on emission spectra can be ignored when under blue light excitation.
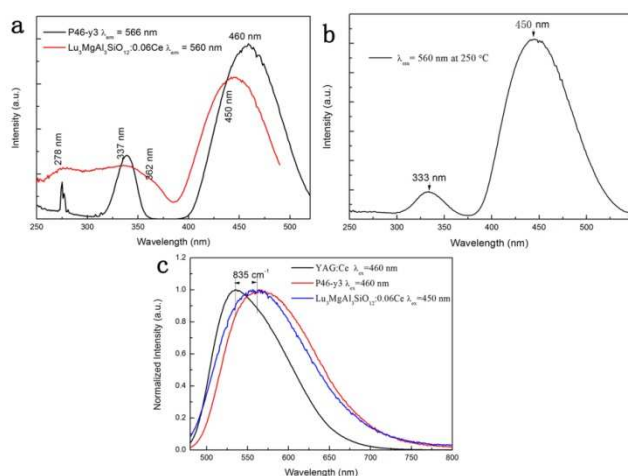
Fig. 4 (a) The room temperature excitation spectra of $Lu_3MgAl_3SiO_{12}$:0.06Ce phosphor and P46-y3 monitored at 560 nm and 566 nm, respectively; (b) The high temperature excitation spectra of $Lu_3MgAl_3SiO_{12}$:0.06Ce phosphor; (c) The normalized emission spectra of YAG:Ce, $Lu_3MgAl_3SiO_{12}$:0.06Ce and P46-y3 phosphors.

3.3 Properties for *w*-LEDs use

While $Lu_3MgAl_3SiO_{12}$:xCe phosphors have redder spectral in comparison to YAG:Ce, the brightness, intensity and room temperature QE must be high for practical use. Thus, it is necessary to find the best concentration of Ce^{3+} in this garnet compound. Fig. 5 shows the PL spectra of different doping concentration x in $Lu_3MgAl_3SiO_{12}$:xCe phosphors. Under 450 nm excitation, all emission spectra show same shape peaked at 560 nm. The intensity increases with the increase of the concentration x first, reaches a maximum value at x=0.06, then decreases due to the concentration quenching effect. The brightness and intensity of optimized $Lu_3MgAl_3SiO_{12}$:Ce phosphor excited by 450 nm can reach 98.9% and 97.5% of that for P46-y3 excited by 460 nm. Besides, the room temperature QE of optimized $Lu_3MgAl_3SiO_{12}$:Ce phosphor is comparable to typical garnet phosphors, and the value is 81.2% in comparison to that of 89.7% for P46-y3.

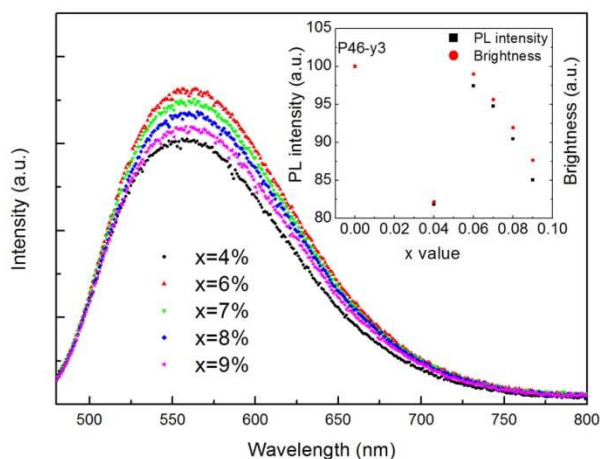Fig. 5 The emission spectra of $Lu_3MgAl_3SiO_{12}$:xCe phosphors. The inset is the PL intensity and brightness of $Lu_3MgAl_3SiO_{12}$:xCe phosphors compared with that for P46-y3.

For application in high power *w*-LEDs, the thermal quenching property is one of the important technological parameters because

it has considerable influence on the light output and color rendering performance, especially for blue LED. Thus, the thermal stability plays an important role in ensuring a high efficiency of phosphor-converted blue chip LEDs.[34-38] Fig. 6 gives temperature-dependent photoluminescence spectra for optimized $Lu_3MgAl_3SiO_{12}$:Ce phosphor. With increase temperature from 20 °C to 250 °C, the shape seems the same with very little blue shift (560 nm in 20 °C *vs* 558 nm for 250 °C, which can be explained by faster quenching of low energy emission band if compared to its high energy counterpart, like in $CaY_2Al_4SiO_{12}$:Ce^{3+} garnet phosphor.[21] This is an agreement with the asymmetric emission band, shown in Fig. 4c). The inset of Fig. 6 is the brightness *vs* temperature for $Lu_3MgAl_3SiO_{12}$:0.06Ce phosphor excited by 450 nm and in comparison to P46-y3 excited by 460 nm. It is clearly seen that the thermal stability of the luminescence of $Lu_3MgAl_3SiO_{12}$:0.06Ce phosphor is greater than that of P46-y3. When the temperature was increased to 150 °C, emission intensity of optimized $Lu_3MgAl_3SiO_{12}$:Ce phosphor dropped to only 81.1% of its initial intensity, while that of P46-y3 decreased to 68.0 %. The higher thermal stability of synthesized optimized $Lu_3MgAl_3SiO_{12}$:Ce phosphor indicates that it can be good candidate yellow phosphor for blue chip LEDs. Also, it is expected that the thermal stability of this new phosphor can be further enhanced by improved preparation conditions, which can restrain apatite structure forming. The better thermal stability of novel garnet phosphor can be explained as following. $Lu_3MgAl_3SiO_{12}$ and YAG have same garnet crystal structure. Ce^{3+} occupies Lu and Y sites. Both are dodecahedral coordination. Thus, we can assume that when these two phosphors undergo high temperature, factors are similar beyond the atom's weight. As Lu is more weight than Y, the agitation range radius R_1 is smaller than R_2, schematic diagram showed in Fig. 7. Larger R causes to more energy lose, resulting in worse thermal stability. From the aspect, if phosphors have same crystal structure, Lu-based phosphors should have better thermal stability than that for other rare-earth ions based phosphors.
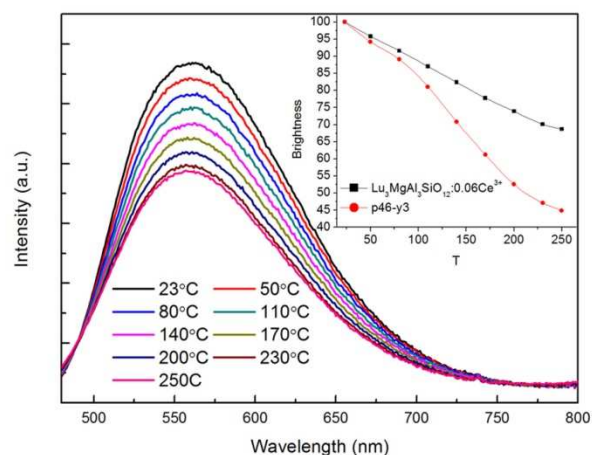

Fig. 6 Photoluminescence behaviors of the optimized $Lu_3MgAl_3SiO_{12}$:Ce phosphor processed at the different temperatures. The inset is the brightness *vs* temperature for optimized $Lu_3MgAl_3SiO_{12}$:Ce phosphor excited by 450 nm and in comparison with that for P46-y3 excited by 460 nm.
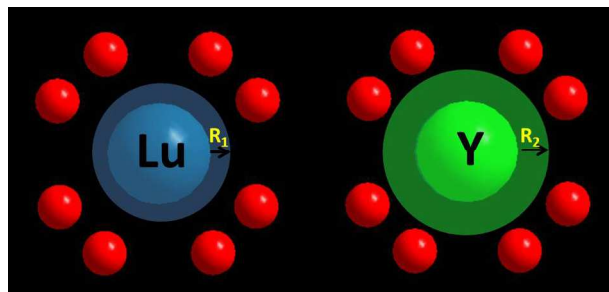
Fig. 7 Schematic diagram for thermal agitation of Lu^{3+} and Y^{3+} based garnet phosphors, R_1 and R_2 are the agitation range radii of Lu^{3+} and Y^{3+} based garnet phosphors, respectively.

The commission International de I'Eclairage (CIE) chromaticity coordinates and CCTs for optimized $Lu_3MgAl_3SiO_{12}$:Ce phosphor, YAG:Ce and P46-y3 phosphors are shown in Fig. 8. ① and ② are excitation wavelength of each phosphor. ③, ④ and ⑤ are the CIE chromaticity coordinates of each other. The connection of excitation wavelength and CIE chromaticity coordinates will meet with blackbody radiation in a bit, which is the CCT value. From this figure, blue LED chip combined with prepared YAG:Ce will get highest CCT, which cannot be accepted by many domain. While this new garnet phosphor, when combined with blue chip LEDs, can give single phosphor convert white light LEDs (pc-*w*-LEDs) with lower CCTs ($\approx$ 5500 K) than that of P46-y3, and introducing high CRI. Above analysis results show optimized $Lu_3MgAl_3SiO_{12}$:Ce phosphor has great potential application in blue chip LEDs.

①:Excitation Wavelength 460 nm
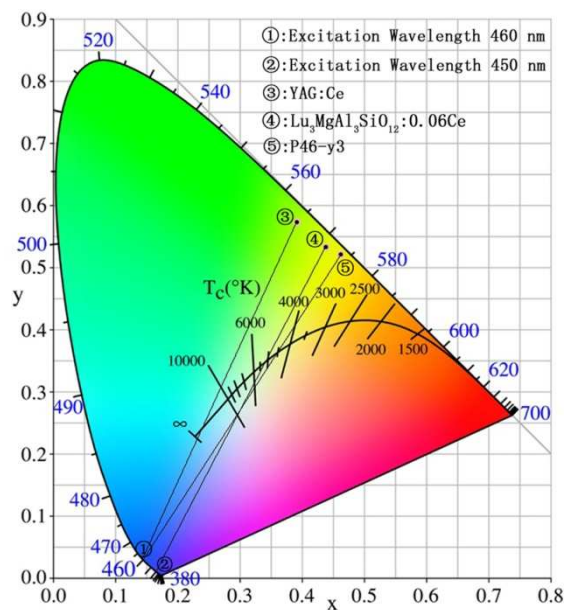②:Excitation Wavelength 450 nm
③:YAG:Ce
④:$Lu_3MgAl_3SiO_{12}$:0.06Ce
⑤:P46-y3

Fig. 8 The CIE chromaticity coordinates and CCTs for optimized $Lu_3MgAl_3SiO_{12}$:Ce, YAG:Ce and P46-y3 phosphors.

4. Conclusion

We have presented the preparation and luminescence characterization of $Lu_3MgAl_3SiO_{12}$:Ce phosphor for blue chip LEDs. XRD Rietveld refinement results show that $Lu_3MgAl_3SiO_{12}$:Ce phosphor is in garnet structure, and Ce^{3+} occupy Lu^{3+} sites on the dodecahedral sites, Mg and Al1 are randomly distributed on the octahedral sites, and Si and Al2 are randomly distributed on the tetrahedral sites. $(Ce/Lu)O_8$ dodecahedron is surrounded by four $(Ce/Lu)O_8$ dodecahedron, four $(Mg/Al1)O_6$ octahedrons and six $(Si/Al2)O_4$ tetrahedrons. The excitation and emission spectra show this new garnet phosphor can be excited efficiently by 450 nm and emit yellow color with higher luminescence intensity and room temperature QE. The temperature-dependent photoluminescence spectra show the optimized $Lu_3MgAl_3SiO_{12}$:Ce phosphor has better thermal stability than commercial YAG:Ce phosphor P46-y3, when the temperature was increased to 150 °C, the emission intensity of only dropped to 81.1% of its initial intensity, while that of P46-y3 decreased to 68.0 %. The CIE chromaticity coordinates suggest that when combined with blue chip, this new garnet phosphor can give single phosphor convert white light LEDs with lower CCTs (5500 K) and high CRI. All of these characterizations indicate the optimized $Lu_3MgAl_3SiO_{12}$:Ce phosphor is a good candidate yellow phosphor for blue chip LEDs.

Authors' Address

a Key Laboratory for Special Function Materials and Structural Design of the Ministry of Education, School of Physical Science and Technology, Lanzhou University, Lanzhou, 730000, China.
b The Key Laboratory of Rare Earth Functional Materials and Applications, Zhoukou Normal University, Zhoukou, 466001, P. R. China.
c Mitsubishi Chemical Group Science and Technology Research Center, Yokohama 227-8502, Japan.

Footnotes

*Corresponding Author: wyh@lzu.edu.cn

Reference

1   T. Suehiro, N. Hirosaki and R. J. Xie, *ACS Appl. Mater. Inter.* 2011, **3**, 811.
2   S. K. Kim, J. W. Lee, H. S. Ee, Y. T. Moon, S. H. Kwon, H. Kwon and H. G. Park, *Opt. Exp.* 2010, **18**, 11025.
3   T. C. Liu, B. M. Cheng, S. F. Hu and R. S. Liu, *Chem. Mater.* 2011, **23**, 3698.
4   Z. Y. Mao and D. J. Wang, *Inorg. Chem.* 2010, **49**, 4922.
5   A. A. Setlur, W. J. Heward, Y. Gao, A. M. Srivastava, R. G. Chandran and M. V. Shankar, *Chem. Mater.* 2006, **18**, 3314.
6   A. A. Setlur, W. J. Heward, M. E. Hannah and U. Happek, *Chem. Mater.* 2008, **20**, 6277.
7   W. B. Im, Y. Kim, N. N. Fellows, H. Masui, G. A. Hirata, S. P. DenBaars and R. Seshadri, *Appl. Phys. Lett.* 2008, **93**, 091905.
8   L. Wang, X. Zhang, Z. D. Hao, Y. S. Luo, X. J. Wang and J. H. Zhang, *Opt. Exp.* 2010, **18(24)**, 25177.
9   H. Yang and Y. S. Kim, J. Lumin. 2008, **128(10)**, 1570.
10 Y. X. Pan, M. M. Wu and Q. Su, *J. Phys. Chem. Solids*, 2004, **65(5)**, 845.
11 Y. R. Shi, Y. H. Wang, Y. Wen, Z. Y. Zhao, B. T. Liu and Z. G. Yang, *Opt. Exp.* 2012, **20(19)**, 21656.
12 Y. S. Lin and R. S. Liu, *J. Lumin.* 2007, **122**, 580.
13 Y. S. Lin, R. S. Liu and B. M. Cheng, *J. Electrochem. Soc.* 2005, **152(6)**, J41.
14 M. M. Shang, J. Fan, H. Z. Lian, Y. Zhang, D. L. Geng and J. Lin, *Inorg. Chem.* 2014, **53(14)**, 7748.

15 R. J. Xie, N. Hirosaki, T. Suehiro, F. F. Xu and M. Mitomo, *Chem. Mater.* 2006, **18 (23)**, 5578.

16 J. W. Li, T. Watanabe, H. Wada, T. Setoyama and M. Yoshimura, *Chem. Mater.* 2007, **19 (15)**, 3592.

17 A. Katelnikovas, H. Bettentrup, D. Uhlich, S. Sakirzanovas, T. Justel and A. Kareiva, *J. Lumin.* 2009, **129**, 1356.

18 Y. F. Liu, X. Zhang, Z. D. Hao, X. J. Wang and J. H. Zhang, *Chem. Commun.* 2011,**47**, 10677.

19 Y. F. Liu, X. Zhang, Z. D. Hao, Y. S. Luo, X. J. Wang and J. H. Zhang, *J. Mater. Chem.* 2011, **21**, 16379.

20 A. Kalaji, P. J. Saines, N. C. George and A. K. Cheetham, *Chem. Phys. Lett.* 2013, **586**, 91.

21 A. Katelnikovas, S. Sakirzanovas, D. Dutczak, J. Plewa, D. Enseling, H. Winkler, A. Kareiva and T. Justel, *J. Lumin.* 2013, **136**, 17.

22 A. Katelnikovas, H. Winkler, A. Kareiva and T. Jüstel, *Opt. Mater.* 2011, **33**, 992.

23 Y. C. Jia, Y. J. Huang, N. Guo, H. Qiao, Y. H. Zheng, W. Z. Lv, Q. Zhao and H. P. You, *RSC Adv.* 2012, **2**, 2678.

24 C. Milanese,V. Buscaglia, F. Maglia and U. Anselmi-Tamburini, Chem. Mater. 2004, 16, 1232.

25 V. Bachmann, C. Ronda and A. Meijerink, *Chem. Mater.* 2009, **21 (10)**, 2077.

26 J. M. Ogiegło, A. Katelnikovas, A. Zych, T. Jüstel, A. Meijerink and C. R. Ronda, *J. Phys. Chem. A*, 2013, **117**, 2479.

27 M. M. Shang, G. G. Li, D. L. Geng, D. M. Yang, X. X. Kang, Y. Zhang, H. Z. Lian and J. Lin, *J. Phys. Chem. C*, 2012, **116 (18)**, 10222.

28 Z. X. Tao, Y. L. Huang and H. J. Seo, *Dalton Trans.* 2013, **42**, 2121.

29 H. Y. Chung, C. H. Lu and C. H. Hsu, *J. Am. Ceram. Soc.* 2010, **93(7)**, 1838.

30 R. Praveen, L. Shi, K. H. Jang, V. Venkatramu, C. K. Jayasankar and H. J. Seo, *J. Alloys Compd.* 2011, **509(3)**, 859.

31 L. X. Wang, M. Yin, C. X. Guo and W. P. Zhang, *J. Rare Earths*, 2010, **28(1)**, 16.

32 W. J. Miniscalco, J. M. Pellegrino and W. M. Yen, *J. Appl. Phys.* 1978, **49**, 6109.

33 X. H. Gong, J. H. Huang, Y. J. Chen, Y. F. Lin, Z. D. Luo and Y. D. Huang, *Inorg. Chem.* 2014, **53(13)**, 6607.

34 W. T. Chen, H. S. Sheu, R. S. Liu and J. P. Attfield, *J. Am. Chem. Soc.* 2012, **134**, 8022.

35 Z. J. Zhang, O. M. ten Kate, A. C. A. Delsing, M. J. H. Stevens, J. T. Zhao, P. H. L. Notten, P. Dorenbos and H. T. Hintzen, *J. Mater. Chem.* 2012, **22**, 23871.

36 Z. J. Zhang, O. M. ten Kate, A. Delsing, E. van der Kolk, P. H. L. Notten, P. Dorenbos, J. T. Zhao and H. T. Hintzen, *J. Mater. Chem.* 2012, **22**, 9813.

37 C. R. Ronda, Luminescence: From Theory to Applications; Wiley-VCH Verlag GmbH & Co. KGaA: Weinheim, 2008.

38 S. Shigeo and M. William, Phosphor Handbook; CRC Press:Washington, DC, 1998.

Dalton Transactions Accepted Manuscript

For Table of Contents Use Only

Novel Ce^{3+} activated Lu$_3$MgAl$_3$SiO$_{12}$ garnet phosphor for blue chip light-emitting diodes with excellent performance

Yurong Shi, Ge Zhu, Masayoshi Mikami, Yasuo Shimomura and Yuhua Wang *
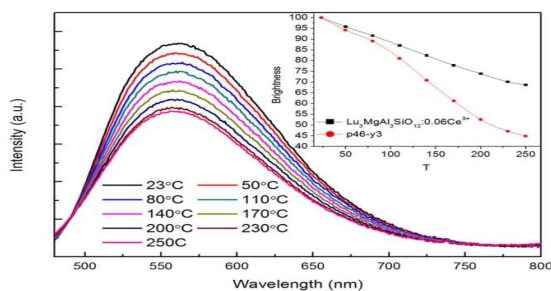
The design, synthesis, and photoluminescence of a novel Lu$_3$MgAl$_3$SiO$_{12}$:Ce^{3+} garnet phosphor for potential warm-white LED applications is reported.